Int J Adv Manuf Technol (2016) 83:157–165
DOI 10.1007/s00170-015-7559-3

ORIGINAL ARTICLE

A novel power skiving method using the common shaper cutter

Erkuo Guo[1] · **Rongjing Hong**[1] · **Xiaodiao Huang**[1] · **Chenggang Fang**[1]

Received: 9 January 2015 / Accepted: 5 July 2015 / Published online: 21 July 2015

Abstract To reduce the skiving cutter cost and make the power skiving more flexible, a novel skiving method is proposed by optimizing the machine setting parameters using a common shaper cutter. First, the mathematical model of power skiving for working an involute cylinder gear was established based on the engagement principle of crossed helical gear. Then, a common shaper cutter profile deviations caused by the cutting angles was derived. By analyzing the relationship between the tooth deviations and the machine setting parameters, a correction method for both flanks power skiving is proposed to correct the machine setting parameter using the principle of linear superposition and the linear regression method. The validity of the correction method for power skiving is numerically demonstrated as working an involute cylinder gear for example. The results show that power skiving process can be achieve by the common shaper cutter and makes the latest technology more flexible and economic.

Keywords CNC machine · Power skiving · Shaper cutter · Correction method

Nomenclature

Σ	Setting angle of the cutter
β_1	Helix angle of gear
β_2	Helix angle of cutter
v	Cutting velocity
v_1	Speed of skiving cutter
v_2	Speed of workpiece
v_{1a}	Axial speed of skiving cutter
v_{1t}	Tangential speed of skiving cutter
v_t	Resultant speed of workpiece
$v_0^{(2)}$	Axial feed of workpiece
ω_1	Angular velocity of skiving cutter
ω_2	Angular velocity of workpiece
$\Delta\omega_1$	Incremental angular velocity of ω_1
m_n	Normal module of tooth
β_1	Helix angle of skiving cutter
β_2	Helix angle of gear
Z_t	Teeth number of cutter
Z_g	Teeth number of gear
i_{21}	Ratio between cutter and gear
a	Center distance between the cutter and workpiece
l_2	Axial incremental movement
φ_1, φ_2	Rotation angles of skiving cutter and workpiece
n_1, n_2	Rotation speeds of skiving cutter and workpiece
(u, θ)	Surface parameters
p	Screw parameter
r_b	Radius of base circle
σ_0	Half angular tooth thickness on the base circle
b	Width of gear
p	Screw parameter of helical gear
γ	Top rake angle
α_e	Top relief angle
Δf_a	Tooth deviation on the top
Δf_f	Tooth deviation in root
$\Delta\Sigma$	Machine setting parameter of setting angle

✉ Rongjing Hong
hongjmst@sina.com

[1] Jiangsu Key Laboratory of Digital Manufacturing for Industrial Equipment and Control Technology, Nanjing Tech University, Nanjing, Jiangsu Province, China

Δa	Machine setting parameter of center distance
Δn	Machine setting parameter of rotation angle
$r^{(1)}$	Cutter tooth position
$r^{(2)}$	Gear tooth position
$r_e^{(2)}$	Gear tooth position deviated from actual tooth
$\delta \boldsymbol{r}_i$	Normal surface deviations
M_{21}	Transformation matrices
$\delta\zeta_j$	Compensations to the polynomial coefficients
$[M_{ij}]$	Sensitivity matrix with respect to the polynomial coefficients

1 Introduction

It has been known that the power skiving process for machining internal gears is multiple times faster than shaping, and more flexible than broaching, due to skiving's continuous chip removal capability. The patent of the skiving process was assigned in the beginning of the twentieth century. However, the method was not implemented at that time because power skiving has always presented a challenge to machines and skiving cutters [1]. With the improvements of CNC technology, latest research demonstrates that power skiving is capable of being a high-productive and flexible alternative to gear manufacture in market [2, 3].

The current developments were initiated at the Institute of Production Science with a numerical method to calculate the tools [4], the power skiving was considered as a contemporary gear pro-machining solution, and the economic and environment friendly aspects of the power skiving process were explained. The subsequent methodical experimental analyses indicated the potential and advantages [5, 6]. Volker [7] established a 3D-FEM model of gear skiving to investigate the kinematical conditions as well as chip formation mechanisms and evaluation of the effects on process reliability. Within such investigation, Hartmut and Olaf [8] proposed a semi-completing skiving method and apparatus for gear power skiving, then [9] they provided a new method to improve the uniformity of load to both flank cutting edges and extend the longest possible tool service life. Li and Chen [10, 11] proposed a slicing technology for cylindrical gears to improve the limitation of current gear machining method for inner gear. Then [12], a design method of error-free spur slice cutter was obtained, and the structure of the rake face was determined according to technological realization of the design, manufacturing, and tool grinding. Besides, Lin [13] and Guo [14, 15] proposed a novel error-free design method for shaper cutter and skiving cutter, respectively. Although they laid a foundation for the study of cutter design, the complex skiving cutter increases the cost and limit the development of power skiving.

Therefore, it is necessary to do some studies on the skiving method. This work aims to propose a novel power skiving method using the common shaper cutter based on adjusting machine setting parameters. Compare with the conventional design method, it is more flexible and economic.

2 Principle of gear power skiving

Skiving is a continuous chip removal method for universal gear manufacturing. In this manufacturing technology, it is performed different from hobbing and sharping. The skiving cutter is placed in a shaft angle with respect to the workpiece; similar to the shaving process, chip building is initiated by the relative velocity between cutter and workpiece. The geometric setup of skiving cutter relative to an internal gear is shown in Fig. 1. Consider that Cartesian coordinate systems $S_1(O_1\text{-}x_1,y_1,z_1)$ and $S_2(O_2\text{-}x_2,y_2,z_2)$ are rigidly connected to the coordinate of workpiece and skiving cutter, respectively. The front view of the generating gear system is shown in the upper graphic, the internal gear is oriented in the coordinate system S_1 with its axis of rotation collinear to the z_1-axes, and the skiving cutter

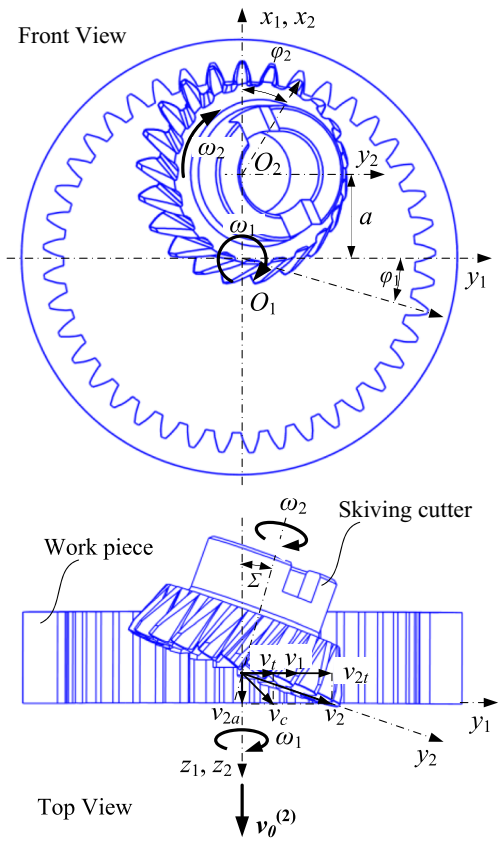

Fig. 1 Kinematical principle of power skiving for an internal cylindrical gear

is oriented in the coordinate system S_2 with its axis of rotation collinear to the z_2-axes. The cutter center is positioned out of the center of xy plane by a radial distance vector a. The pitch circles of the gear and cutter contact tangentially at the lowest point of the pitch circle. The top view, which shows the tool shaft angle Σ between workpiece axes and skiving cutter axes, is drawn below the front view. In case of spur gear, the stroke motion $v_0^{(2)}$ is directed in line with the z_1-axis. The workpiece and cutter perform with an angular velocity ω_1 and ω_2, respectively. When the axial feed motion $v_0^{(2)}$ is increasing, the workpiece rotates about z_1-axes by φ_1 and the cutter rotates about z_2-axes by φ_2.

The cutting velocity v_c results form positioning constraints during the rolling of the generation train and uses the resulting relative movement of workpiece and skiving cutter. Therefore, the cutting velocity depends on the number of revolution of the generation train and the shaft angle. As Fig. 1 shown, the cutter velocity v_2 is divided into the axial speed v_{2a} and tangential velocity v_{2t}. Then, the tangential velocity v_{2t} and the workpiece v_1 result in the resultant tangential velocity v_t. Consequently, the cutting velocity v_c results from the axial speed v_{2a} and the resultant tangential speed v_t.

In case of working a helical gear, the stroke motion is oriented in z_1-axis direction, but an incremental angular velocity $\Delta\omega_1$, which depends on the axial feed, has to be added to ω_1. The incremental angular velocity of workpiece, $\Delta\omega_1$ is determined by the following equation:

$$\Delta\omega_1 = \frac{2v_0^{(2)}\sin\beta_1}{m_n Z_g} \tag{1}$$

where $v_0^{(2)}$ is the axial stroke feed, m_n is the normal module of tooth, Z_g is the tooth number of workpiece, and Z_t is the tooth number of skiving cutter.

Therefore, the relationship between the angular velocity of workpiece and cutter and axial feed satisfies the following relation:

$$\omega_1 = \frac{Z_t}{Z_g}\omega_2 - \frac{2v_0^{(2)}\sin\beta_1}{m_n Z_g} \tag{2}$$

On the contrary, if the workpiece provides the incremental movement, the relation can be represented as

$$\omega_2 = \frac{Z_g}{Z_t}\omega_1 - \frac{2v_0^{(2)}\sin\beta_1}{m_n Z_t} \tag{3}$$

3 Tooth deviation analysis of power skiving

According to the gear principle, the swept surface family engages with the gear tooth surface, so there are no error on the tooth profile if the cutting blade projected on the base plane is involute. Actually, in order to improve the cutting condition, the shift shaper cutter is designed as the tapered teeth with the top rake angle γ and top relief angle α_e. When the top rake angle γ=0, the tooth profile are error-free on the rake plane. When the rake angle γ> 0, the tooth profile deviate from the projection of the intersecting lines between the involute helicoid and the cutter blade. Taking the intersection plane on the pitch circle as the reference plane, the thickness on the top increase by Δf_a while the thickness on the root decrease by Δf_f.

As shown in Fig. 2, AB is the theoretically involute with the pressure angle α and base radius r_b, CD is the projection of cutter blade with the pressure angle α_0 and the base radius r_{b0}. If CD rotates ε about O_0 to match point G on the pitch circle,

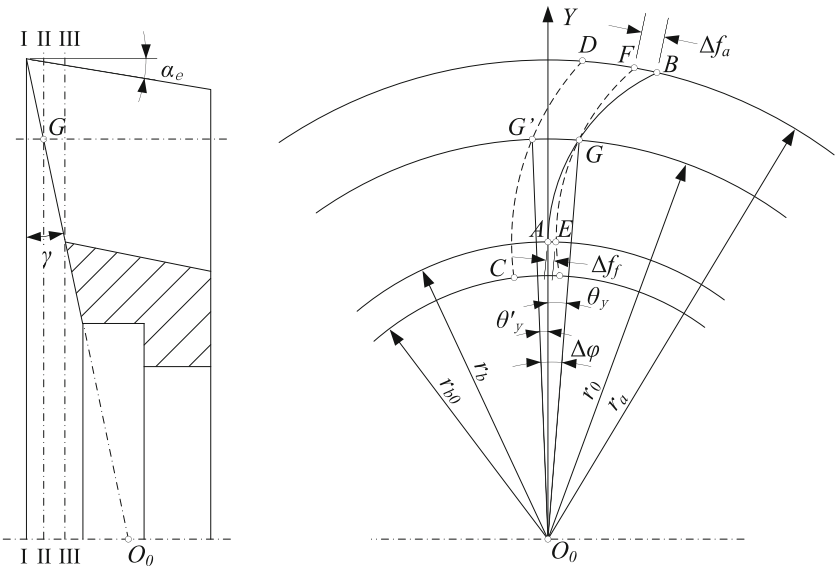

Fig. 2 Tooth deviation of the shaper cutter

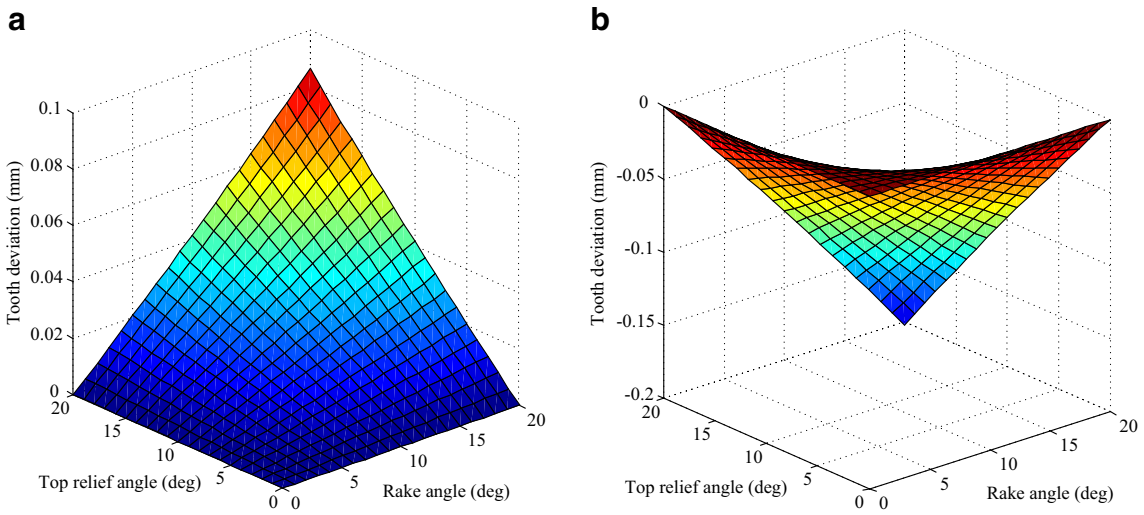

Fig. 3 Illustration of tooth deviations due to the rake angle and top side angle **a** on the top and **b** in root

then *FB* represents the tooth deviation Δf_a on the top and *AE* represents the tooth deviation Δf_f on the root.

Assuming that the involute starts at the point A on the coordinate O_0Y, the polar equation of the involute is expressed as

$$\theta_y = \mathrm{inv}\alpha_y \tag{4}$$

where $\cos\alpha_y = \frac{r_{b0}}{r_y}$.

The rotation angle $\Delta\varphi$ rotates from *G'* to *G* is determined as

$$\Delta\varphi = \frac{\Delta b\tan\beta_y}{r_y} = \frac{r_y\tan\gamma\tan\beta_0}{r_0} = \frac{r_y\tan\gamma\tan\alpha_0\tan\alpha_e}{r_0} \tag{5}$$

where $\Delta b = r_y \tan\gamma$, β_0 is the helix angle on pitch circle, and $\tan\beta_0 = \tan\alpha_0 \tan\alpha_e$.

The projection of cutter blade *CD* can be represented by

$$\theta'_{y0} = \theta_{y0} - r_y\left(\frac{\tan\gamma\tan\alpha_0\tan\alpha_e}{r_0}\right) = \mathrm{inv}\alpha_{y0} - r_y{\cdot}K \tag{6}$$

where $K = \frac{\tan\gamma\tan\alpha_0\tan\alpha_e}{r_0}$, $\cos\alpha_{y0} = \frac{r_{b0}}{r_y}$.

Combining the angle coordinate $\theta_0' = \mathrm{inv}\alpha_0 - r_0{\cdot}K$ on the projection point *G'* with the angle coordinate $\theta = \mathrm{inv}\alpha$ on the theoretical point *G*, yields the rotation angle ε in the pitch circle

$$\varepsilon = \theta'_0 - \theta = (\mathrm{inv}\alpha_0 - \mathrm{inv}\alpha) - r_0{\cdot}K \tag{7}$$

The equation of the cutting blade after projecting on the reference plane can be represented by

$$\begin{aligned}\theta''_{y0} &= \theta'_{y0} - \varepsilon = \mathrm{inv}\alpha_{y0} - r_y{\cdot}K - (\mathrm{inv}\alpha_0 - \mathrm{inv}\alpha) + r_0{\cdot}K \\ &= \mathrm{inv}\alpha_{y0} - (\mathrm{inv}\alpha_0 - \mathrm{inv}\alpha) - (r_y - r_0)K\end{aligned} \tag{8}$$

Then, we obtain the angle difference between the projection involute and the desired involute by the following equation

$$\Delta\theta_y = \theta''_{y0} - \theta_y = (\mathrm{inv}\alpha_{y0} - \mathrm{inv}\alpha_y) - (\mathrm{inv}\alpha_0 - \mathrm{inv}\alpha) - (r_y - r_0)K \tag{9}$$

Consequently, the error Δf_y from the theoretical value represent the tooth deviation

$$\Delta f_y = r_y\left[(\mathrm{inv}\alpha_{y0} - \mathrm{inv}\alpha_y) - (\mathrm{inv}\alpha_0 - \mathrm{inv}\alpha) - (r_y - r_0)K\right] \tag{10}$$

For analyzing the relationship between the top rake angle and top relief angle, a numerical example is given in Fig. 3 and Table 1 when the shaper cutter parameters are as follows: m_n= 3 mm, z_1=31, and α=20°. The tooth deviations are increased

Table 1 Top rake angle and top relief angle corresponding to the tooth deviation

Top rake angle γ	Tooth deviation (μm)		Top relief angle α_e	Tooth deviation (μm)	
	tooth top Δf_a	tooth root Δf_f		tooth top Δf_a	tooth root Δf_f
5°	−15.9	+8.6	3°	−7.9	+4.3
10°	−32.1	+17.4	6°	−15.9	+8.6
15°	−48.8	+26.4	9°	−24.0	+13.0
20°	−66.2	+35.8	12°	−32.2	+17.4

Shaper cutter parameters: m_n=3 mm, z_1=31, α=20°, γ=5°, α_e=6°

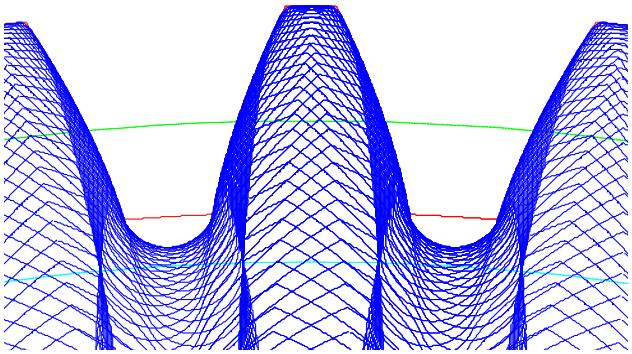

Fig. 4 Gear tooth profile performed by skiving cutter

as the top rake angle and top relief angle are increased. For example, if the rake angle γ=5° and top side angle α_e=6°, the tooth deviations on the top Δf_a and root Δf_f are −15.9 and + 8.6 μm, respectively. The cutter tooth deviations caused by the rake angle γ and relief angle α_e are copied to the gear tooth deviations where the profile is over-cut on the top and less-cut in root. Besides, consider a better cutting condition, the bigger rake angle and top side angle are required that it inevitably leads to a larger tooth deviation. Therefore, it is necessary to correct the cutter tooth deviations caused by the cutter angles. The present methods are focus on the design and manufacture of the theoretical error-free skiving cutter. The specially made cutter, which is more complex and expensive, makes the power skiving technology hard to widely apply. Therefore, we propose a flexible and economic skiving method to correct the tooth deviation using the common shaper cutter based on adjusting machine setting parameters.

4 Correction method for tooth deviation

Using the numerical simulation in early study, the tooth deviations are sensitive to the setting parameters including the cutter setting angle error $\Delta\Sigma$, cutter setting displacement error Δa, and synchronous error Δn. Next, we discuss the influence of the above setting errors in skiving.

4.1 Establish the tooth surface with setting errors

According to the gear principle [16, 17], assuming that the cutter tooth surface is represented in coordinate system S_1 in two-parametric form $r^{(1)}(u_1,\theta_1)$, the transformation matrices S_1 to S_2 give the gear tooth surface $r^{(2)}(u_2,\theta_2;\Sigma,a,n_1,n_2)$ in coordinate system S_2

$$r^{(2)}(u_2,\theta_2;\Sigma,a,n_1,n_2) = M_2 M_\Sigma M_1 r^{(1)}(u_1,\theta_1) \tag{11}$$

where $M_2 = \begin{pmatrix} \cos\varphi_2 & -\sin\varphi_2 & 0 & 0 \\ \sin\varphi_2 & \cos\varphi_2 & 0 & 0 \\ 0 & 0 & 1 & -l_2 \\ 0 & 0 & 0 & 1 \end{pmatrix}$, $M_\Sigma = \begin{pmatrix} 1 & 0 & 0 & a \\ 0 & \cos\Sigma & -\sin\Sigma & 0 \\ 0 & -\sin\Sigma & \cos\Sigma & 0 \\ 0 & 0 & 0 & 1 \end{pmatrix}$, $M_1 = \begin{pmatrix} \cos\varphi_1 & -\sin\varphi_1 & 0 & 0 \\ \sin\varphi_1 & \cos\varphi_1 & 0 & 0 \\ 0 & 0 & 1 & 0 \\ 0 & 0 & 0 & 1 \end{pmatrix}$,

φ_1 is the rotation angle of cutter, φ_2 is the rotation angle of gear, and a, Σ, and l_2 represent the center distance between the cutter and workpiece centers, the setting angle of the cutter, and axial movement along the workpiece axis, respectively. Figure 4 shows the gear tooth profile performed by skiving cutter using the established mathematical model of tooth surface.

Consider the setting errors are expressed as δ_k=[$\Delta\Sigma$, Δa, Δn], the actual setting parameters can be represented as the equations

$$\begin{cases} \Sigma' = \Sigma + \Delta\Sigma \\ a' = a + \Delta a \\ n_1' = n_1 + \Delta n \end{cases} \tag{12}$$

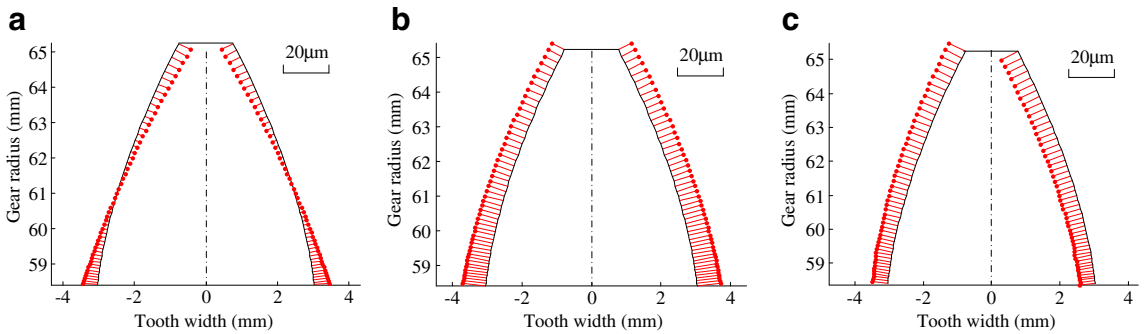

Fig. 5 The relationship between micro-small setting errors and tooth deviations **a** $\Delta\Sigma$=+0.2°, **b** Δa=+0.05 mm, and **c** Δn=+0.05 r/min

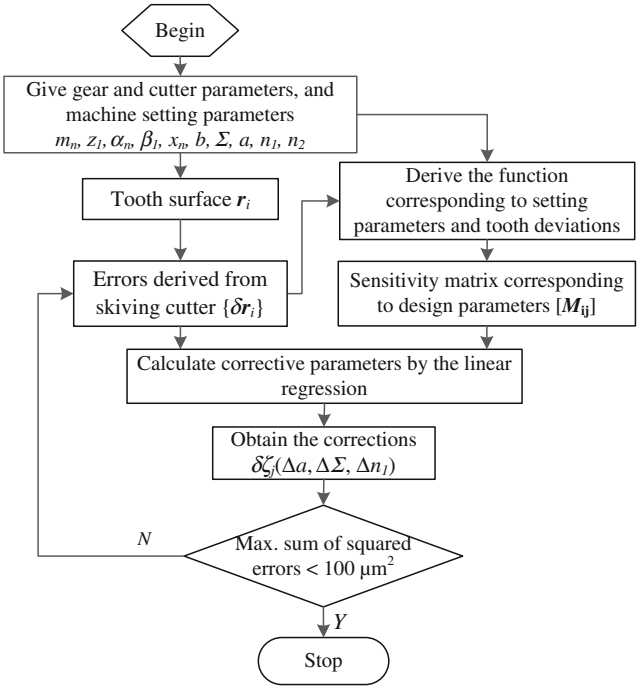

Fig. 6 Flow chart for the correction method

Thus, the gear tooth surface after adjusting parameters may be represented as

$$r_e^{(2)}\left(u_2,\theta_2;\Sigma',a',n_1',n_2\right)=M_2M_\Sigma M_1 r^{(1)}(u_1,\theta_1) \quad (13)$$

Equations (11) and (13) are the parametric expressions of tooth surface with the variable u_2, θ_2, n_1, and n_2. Since $n_1 = i_{12}n_2$, the normal and coordinate of any point on the tooth surface can be derived by the discrete variables. Compared with the theoretical tooth profile without setting error, the profile deviations can be obtained and its parametric equation is expressed as

$$\{\delta r_i\}=r_e^{(2)}\left(u_2,\theta_2;\Sigma',a',n_1',n_2\right)-r^{(2)}(u_2,\theta_2;\Sigma,a,n_1,n_2) \quad (14)$$

4.2 Tooth deviation analysis

In order to achieve the correlated function of setting errors and tooth deviations, the micro errors are given as the initial value for the accumulated error of individual setting error. Therefore, we suppose the setting angle error, setting displacement error, and the rotate speed setting error are +0.05 mm, +0.2°, and +0.05 r/min, respectively.

Figure 5 presents the amplified drawings of profile normal deviation performed by the given setting angle error, displacement setting error, and rotate speed setting error. The trend of profile deviations of angle setting error and displacement setting error indicates that the tooth deviations distribute symmetrically on both the right and left flanks (see Fig. 5a, b). The trend of profile deviations of rotate speed error indicates that the tooth deviations distribute asymmetrically, but the absolute value of deviations are equal on the right and left flank (see Fig. 5c).

Recall that the gear tooth deviations are over-cut on the top and less-cut in root, which are similar to the tooth deviations caused by the sum of angle setting error and displacement setting error. Therefore, the gear tooth deviations can be corrected using the principle of linear superposition with respect to individual tooth deviation of the three setting parameters.

4.3 Compensation method by solving sensitivity coefficients matrix

In order to meet the requirement of skiving precision, we propose an error compensation method based on solving sensitivity matrix with respect to the polynomial coefficients. Since the setting errors are minimum, the higher order terms in polynomial can be neglected, so we assume the total deviation of tooth satisfy the principle of linear superposition with respect to individual tooth deviation of different setting error. The numerical examples demonstrate that the sum of individual tooth deviation of different setting error is equal to the

Fig. 7 Part of the calculation results in solving sensitivity coefficients matrix

before correction δ_k		normal vector $\boldsymbol{n}$ on tooth flanks				sensitive coefficient matrix $[M_{ij}]$			after correction δ_k'	
δ_L	δ_R	n_{x_L}	n_{y_L}	n_{x_R}	n_{y_R}	a_Σ	a_a	a_n	δ_L'	δ_R'
−15.92	−15.92	0.4538	0.8911	−0.4538	0.8911	0.6635	0.2654	< 0.0001	0.33	0.33
−15.45	−15.45	0.4472	0.8944	−0.4472	0.8944	0.6505	0.2602	< 0.0001	0.34	0.34
−13.93	−13.93	0.4406	0.8977	−0.4406	0.8977	0.6410	0.2564	< 0.0001	0.36	0.36
⋮	⋮	⋮	⋮	⋮	⋮	⋮	⋮	⋮	⋮	⋮
1.54	1.54	0.2835	0.9590	−0.2835	0.9590	0.0770	0.0308	< 0.0001	1.08	1.08
⋮	⋮	⋮	⋮	⋮	⋮	⋮	⋮	⋮	⋮	⋮
7.48	7.48	0.1183	0.9930	−0.1183	0.9930	−0.4945	−0.1978	< 0.0001	0.56	0.56
8.09	8.09	0.1110	0.9938	−0.1110	0.9938	−0.4995	−0.1998	< 0.0001	0.54	0.54
8.61	8.61	0.1037	0.9946	−0.1037	0.9946	−0.5035	−0.2014	< 0.0001	0.52	0.52

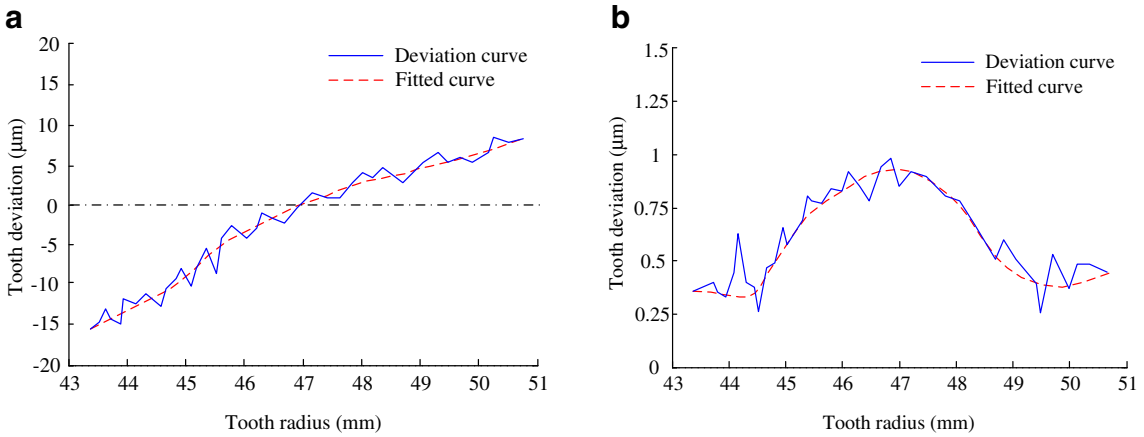

Fig. 8 Tooth deviations **a** before correction and **b** after correction

amount of tooth deviation of composite setting error, and it verify the correctness of assumptions of the linear superposition principle.

The skived tooth surface can be expressed as a function of parameters (u and Σ), which are derived from Eq. (11) and the meshing equation for the generated surface. According to differential geometry, the surface variation vector is as follows in Eq. (15), where ζ_j indicates the polynomial coefficients and q is the number of polynomial coefficients.

$$\delta r = \frac{\partial r}{\partial u}\delta u + \frac{\partial r}{\partial \Sigma}\delta\Sigma + \sum_{j=1}^{q}\frac{\partial r}{\partial \zeta_j}\delta\zeta_j \tag{15}$$

Table 2 Basic parameters for power skiving process in the numerical example

Items		Units
(I) Workpiece data (helical gear)		
Tooth number Z_g	51	-
Module m_n	3	mm
Pressure angle α_n	20	deg
Helix angle β_2	20	deg
Addendum circle d_a	155.319	mm
Dedendum circle d_f	168.819	mm
Gear width b	40	mm
(II) Cutter data (spur shaper cutter)		
Tooth number of cutter Z_t	21	-
Module m_n	3	mm
Top rake angle γ	5	deg
Top relief angle α_e	6	deg
Outside diameter d_2	71.520	mm
(III) Machine setting data		
Shaft angle Σ	20	deg
Setting distance a	112.909	mm
Rotation of cutter n_1	1942.857	r/min
Rotation of gear n_2	800	r/min

Because vectors $\frac{\partial r}{\partial u}$ and $\frac{\partial r}{\partial \Sigma}$ are both perpendicular to the tooth normal, taking the inner product of both sides of the above equation with the tooth normal gives the following simplified normal tooth variation:

$$\delta r\cdot n = \left(\frac{\partial r}{\partial u}\delta u + \frac{\partial r}{\partial \Sigma}\delta\Sigma + \sum_{j=1}^{q}\frac{\partial r}{\partial \zeta_j}\delta\zeta_j\right)\cdot n = \sum_{j=1}^{q}\left(\frac{\partial r\cdot n}{\partial \zeta_j}\right)\delta\zeta_j \tag{16}$$

The normal tooth variations at the topographical grid points may then be written in matrix form:

$$\begin{Bmatrix}\delta r_1\\ \vdots\\ \delta r_p\end{Bmatrix} = \begin{Bmatrix}\frac{\partial r_1}{\partial \zeta_1}n_{11} & \cdots & \frac{\partial r_1}{\partial \zeta_q}n_{1q}\\ \vdots & \ddots & \vdots\\ \frac{\partial r_p}{\partial \zeta_1}n_{p1} & \cdots & \frac{\partial r_p}{\partial \zeta_q}n_{pq}\end{Bmatrix}\begin{Bmatrix}\delta\zeta_1\\ \vdots\\ \delta\zeta_q\end{Bmatrix} \tag{17}$$

That is, $\{\delta r_i\}=[M_{ij}]\{\delta\zeta_j\}(i=1,\cdots,p;j=1,\cdots,q)$ where n represents the tooth normal, r_i is the expression of tooth surface, δr_i represents the normal surface deviations, $\delta\zeta_j$ is the compensations to the polynomial coefficients, and $[M_{ij}]$ is the sensitivity matrix with respect to the polynomial coefficients.

The steps of the method are as follows:

1. Construction of the sensitivity matrix $[M_{ij}]$, by the added small amount in the polynomial coefficients and their corresponding normal deviations of the surface points, the sensitivity matrix $[M_{ij}]$ can be constructed by Eq. (17). Then, the sensitivity matrix is provided as the transformation matrix for the following calculation;.
2. Obtain the tooth deviations $\{\delta r_i\}$ from simulated flank data or on-machine gear measurements;
3. Solve the compensations $\delta\zeta_j(\Delta a, \Delta\Sigma, \Delta n_1)$ by using linear regression method. Because the number of polynomial coefficients j is smaller than the number i, so Eq. (19) is overdetermined, the compensations can be approximated using a linear regression technique like the least squares method:

Table 3 Tooth deviations and machine setting parameters before and after correction

Cutter parameters	Tooth deviation before correction (μm)		Tooth deviation after correction (μm)		Machine setting parameters		
m_n=3 mm, z_0=21, α=20°, γ=5°, α_e=6°	Tooth top Δf_a	Tooth root Δf_f	Tooth top Δf_a	Tooth root Δf_f	$\Delta\Sigma$ (°)	Δa (mm)	Δn (r/min)
	−15.9	+8.6	+0.4	+0.3	−0.2	+0.005	0

$$\delta\zeta_j = \left(M_{ij}{}^T M_{ij}\right)^{-1} M_{ij}{}^T \{\delta r_i\} \tag{18}$$

4. Correction of the tooth deviation by the derived compensations $\delta\zeta_j(\Delta a, \Delta\Sigma, \Delta n_1)$ to control the machine NC system.

In the numerical example, the sensitivity matrix is obtained using the normal flank deviations of 120 grid points (6×10 topographic points, both flank sides). When the sum of squared errors (topographic points) are less than 100 μm^2, the compensations $\delta\zeta_j(\Delta a, \Delta\Sigma, \Delta n_1)$ can be obtained finally (Fig. 6).

5 Numerical example and discussion

A numerical example applies the proposed compensation method to correct the tooth deviations of both flanks. Table 2 gives the basic parameters of skiving cutter and workpiece. The skiving cutter is a common shaper cutter, the tooth deviation are −15.9 μm on the top and +8.6 μm in root, respectively, due to the top rake angle γ= 5° and the top relief angle α_e= 6°.

Substituting the given deviations $\{\delta_i\}$ and the sensitivity matrix M_{ij} into Eq. (18), the compensations to the polynomial coefficients can be calculated by ζ_a=−0.005 mm, ζ_Σ=−0.2°, ζ_{n1}=0. Part of the calculation results in solving sensitivity coefficients matrix, including tooth deviations before correction δ_k, normal in the transverse plane n, sensitivity coefficients matrix M_{ij}, and tooth deviations after correction δ'_k, are presented in Fig. 7.

Based on the calculated compensations, the setting parameters are adjusted in the process of power skiving. Before the correction, the tooth deviation are −15.9 μm on the top and + 8.6 μm in root, see in Table 3. After the correction, the maximum tooth deviation is less than 1 μm that meet the requirement of high-precision skiving. Subsequently, as the figures illustrate in Fig. 8, the proposed correction method efficiently reduces the tooth deviations caused by the cutter angles using a common shaper cutter in power skiving process.

6 Conclusions

This paper established a mathematical model of the power skiving for machining involute cylinder gears and obtained the common shaper cutter profile deviations caused by the top rake angle and top relief angle. On this basis, we proposed a novel skiving method by optimizing the machine setting parameters using a common shaper cutter. This method assumed that machine setting parameters corresponding to the amount of tooth deviation was linear superposition; by constructing the sensitive coefficient matrix, the optimal machine setting parameters can be calculated using a linear regression method. The common shaper cutter was applied rather than the specialized skiving cutter with a complicated profile used in the traditional skiving process of working both flanks. Therefore, the novel power skiving method is more flexible and economic by adjusting the machine setting parameters. Besides, the skiving method and correction models presented in this study have generality, which can be used to involute spur gears, helical gears, and non-involute cylinder gears. These studies will be performed in next experiment study to meet the requirement of gear power skiving.

Acknowledgment This work supported by the National Natural Science Foundation (No.51175242), China.

References

1. Jin J (1962) The principle of gear turning and experimental results, Xi'an Jiaotong University, 2: 69–97
2. Kobialka C (2012) Contemporary gear pre-machining solutions, AGMA No.12, FTM11, ISBN: 987-1-61481-042-1
3. Stadtfeld H (2014) Power skiving of cylindrical gears on different machine platforms. Gear Tech 31(1):52–62
4. Spath D, Huhsam A (2002) Skiving for high-performance machining of periodic structures. Ann CIRP 51(1):472–475
5. Fleischer J, Bechle A, Kuhlewein C (2006) Process development of skiving-a highly productive gearing process. CIRP January Meeting, Presentation STC-C, Paris
6. Fleischer J, Bechle A, Kuhlewein C (2006) High performance gearing by skiving. CIRP 2nd International Conference on High Performance Cutting (HPC), Canada
7. Volker S, Chirsttoph K, Hermann A (2011) 3D-FEM modeling of gear skiving to investigate and chip formation mechanisms. Adv Mater Res 223:46–55
8. Hartmut M, Olaf V (2012) Robust method for skiving and corresponding apparatus comprising a skiving tool. US patent, 20120328384A1
9. Hartmut M, Olaf V (2013) Semi-completing skiving method and device having corresponding skiving tool for executing a semi-completing skiving method. US patent, 20130071197A1
10. Li J, Chen XC, Zhang HY (2011) Slicing technology for cylindrical gears. Chin J Mech Eng-En 47(19):193–198
11. Chen XC, Li J, Lou BC (2013) A study on the design of error-free spur slice cutter. Int J Adv Manuf Technol 68(4):727–738

12. Chen XC, Li J, Peng W (2014) A study on the grinding of the major flank face of error-free spur slice cutter. Int J Adv Manuf Technol 72(2):425–438
13. Lin SW, Han CS, Tan JB (2010) Mathematical models for manufacturing a novel gear shaper cutter. J Mech Sci Technol 24: 383–390
14. Guo EK, Hong RJ, Huang XD (2014) Research on the design of skiving tool for machining involute gears. J Mech Sci Technol 20(12):5017–5115
15. Guo EK, Hong RJ, Huang XD (2015) Research on the cutting mechanism of cylindrical gear power skiving. Int J Adv Manuf Technol 79(1):541–550
16. Wu XT (2009) Principle of gearing, 2nd edn. Xi'an Jiaotong University Press, China
17. Litvin FL, Fuentes A (2004) Gear geometry and applied theory (2th ed). Cambridge University Press, New York